CFSRC COLLOQUIUM

Proceedings of the Cold-Formed Steel Research Consortium Colloquium
20-22 October 2020 (cfsrc.org)

Analytical study of unstiffened extended end-plate connections produced from austenitic stainless steel

Mohammed M. Eladly[1]

Abstract

Based on the numerical data of 66 unstiffened stainless steel beam-to-column extended end-plate (EEP) joints, a straightforward analytical method, for predicting the moment-rotation (M-Φ) response of this connection type, was developed and validated. The joint configurations employed to formulate the analytical equations cover a broad range of parameters having significant influence on the performance of this connection typology widely-utilized in steel buildings in seismic zones. To derive the equations, Richard and Abbott expression for the relationship between the moment and rotation, was adopted. This expression takes into account the strain-hardening characteristics and thus is capable of accurately predicting the response of ductile materials having considerable strain hardening such as stainless steel. The results showed that the proposed analytical model has been able to provide accurate predictions of the moment-rotation behavior of connections, with an average error less than 5% in estimating the maximum moment capacity. Finally, an additional evaluation of the suggested model was performed using finite element results for connection configurations other than those used in the calibration of the model. The further assessment demonstrated the high level of accuracy of the developed formulas over a wide range of parameters' values. These suggested formulas can act as a simple analytical technique for predicting the entire moment-rotation response of unstiffened stainless steel EEP joints, using readily-obtainable geometric and material parameters.

1. Introduction

Despite the great effect of connections on the overall behavior of frames [1-3], only a tiny percentage of investigations into structural stainless steel have concentrated on the joints' behavior. The majority of these studies (i.e. studies on stainless steel joints) were performed on lap joints [4-9], while the studies on beam-to-column connections are limited [10-12]. Such investigations into beam-to-column connections are vital for the assessment of the current design provisions for stainless steel connections (in Eurocode 3 [13,14], and other international structural design codes) which copy those of carbon steel joints, without entirely taking into consideration the ductile response of stainless steel.

Extended end-plate (EEP) connections have got wide popularity among the various typologies of beam-to-column joints used in the construction industry, due to their relatively low cost, and the ease of their fabrication and erection. Studies on carbon steel EEP joints [15-16] showed that this type of connection can offer almost the same initial stiffness and maximum moment capacity of fully-welded connections, but with greater ability to dissipate seismic energy, which leads to a better performance from a structural standpoint. Nonetheless, until now, there is no thorough investigation examining the response of this promising connection typology when produced from stainless steel.

In this paper, finite element (FE) results for stainless steel extended end-plate beam-to-column connections were utilized to develop an analytical model capable of estimating the moment-rotation behavior of this connection type. The accuracy of that suggested model was further assessed depending on numerical data for joint configurations different from those considered to formulate the analytical equations.

2. Finite element model

Based on the simplified FE model suggested by the author in a previous study [17], the finite element data, for 66 unstiffened stainless steel EEP joints, used to calibrate the analytical equations proposed in the present paper, was generated (using the commercial FE analysis software ABAQUS [18]). The model's capability to mimic the behavior of stainless steel bolted joints has already been verified against experimental data in [17] and thus, is not repeated

[1] PhD Student, Department of Civil and Systems Engineering, Johns Hopkins University, Baltimore, MD, USA, eladly@jhu.edu

herein. Nevertheless, for convenience, a summary of the model's structure is provided in the present section.

Four-node stress/displacement shell elements with reduced integration (S4R) were used for all connection parts. To consider the nonlinearity associated with large deformations that beam-to-column bolted joints can suffer from, nonlinear geometry was taken into consideration. CARTESIAN elements [18] were adopted to simulate stainless steel bolts, with "Elasticity and Plasticity" behaviors defined in the bolt axial and shear force directions. To prevent the undue local inelastic deformations at the connectors' nodes, "Rigid Body" constraints [18] were employed. For the contact relationships between the non-welded components of joints (e.g. between beam flange and angles), surface-to-surface contact was utilized, with "Hard" contact relationship in the normal direction and "Coulomb friction" formulation for the tangential interaction. In order to simulate the behavior of stainless steel material, the two-stage Ramberg-Osgood model [19] was used.

3. Analytical model

Depending on the numerical results of 66 unstiffened stainless steel extended end-plate connections, an analytical model for predicting the *M-Φ* response of these joints was suggested. To develop this model, the four-parameter model proposed by Richard and Abbott [20], for M-Φ relationships, was used. Richard and Abbott model is suitable for the current study as it can incorporate the strain-hardening characteristics of ductile materials such as stainless steel.

3.1 Description of Richard-Abbott model

Richard and Abbott [20] proposed a nonlinear mathematical equation for the relationship between the moment (*M*) and rotation (*Φ*). This equation is applicable to various connection configurations with different types of responses including strain hardening. Four parameters [i.e. K_i (initial stiffness), K_p (plastic stiffness), M_o (reference moment), and *N* (curve shape factor)] are included in the Richard-Abbott equation, (Equation 1). Figure 1 presents the definition of the four parameters on a standard moment-rotation curve.

$$M = \frac{(K_i - K_p)\phi}{\left(1 + \left|\frac{(K_i - K_p)\phi}{M_O}\right|^N\right)^{1/N}} + K_p\phi \tag{1}$$

3.2 Four parameters' functions: development and verification

Based on Richard and Abbott formula [20] shown in Equation 1, four parameters are needed to estimate the moment-rotation response of connections (i.e. K_i, *Kp*, M_o, and *N*). Hence, an equation for each of these parameters must be developed, in order to mathematically estimate the complete *M-Φ* response of joints.

Using nonlinear regression analysis of numerical data for 66 stainless steel EEP connections and after taking into consideration various function types, formulas for K_i, *Kp*, M_o, and *N* were suggested (Table 1) in terms of key geometric and material properties (including: thickness of end-plate (t_p); thickness of column flange (t_{fc}); horizontal bolts gauge (*g*); the vertical distances between the bolt rows in tension and the centerline of the beam compression flange (Z_1 and Z_2); depth of beam (*d*); diameter of bolts (*D*); modulus of elasticity (*E*); the nominal yield stress ($\sigma_{0.2}$); and the ultimate stress (σ_u)).

Using the suggested formulas listed in Table 1, the four parameters for the 66 EEP joints were determined. As provided in Table 2, the analytical data showed a good correlation with numerical results with arithmetic mean lying between 0.992 and 1.018 and *COV* between 6.1% and 9.9%.

Figure 2 depicts comparisons between the finite element and analytical four parameters for the 66 joints. From the figure, it is clear that the accuracy of the suggested functions is greater in the case of initial stiffness than in the case of plastic stiffness (Figure 2(a)). This is due to the uncertainties involved in the inelastic behavior of joints, resulting from the nonlinear material response and complex contact relationships. Regarding M_o and *N*, most of their numerical/analytical ratios range from 1.1 and 0.9, which demonstrates very good agreement between FE and analytical reference moment and curve shape parameter (Figure 2(b)).

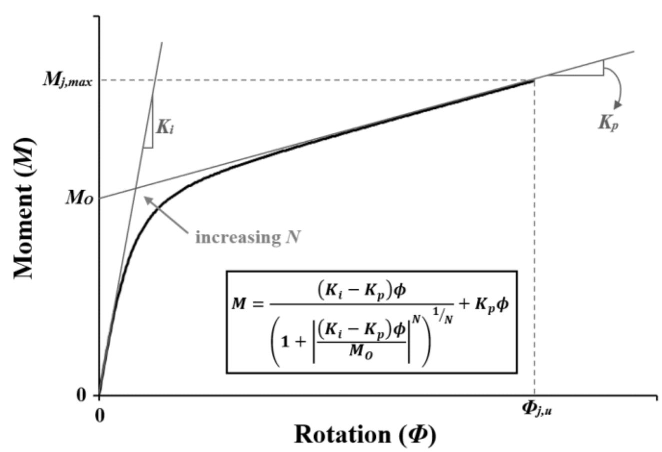

Figure 1: Richard-Abbott [20] formula for defining *M-Φ* relationships

Table 1: Four parameters' formulas for unstiffened stainless steel EEP connections

	Parameter	Unit	Function	
Unstiffened	K_i	*kN.m/rad*	$1.24 \times 10^{-5} \times t_p^{0.809} \times t_{fc}^{0.305} \times g^{-0.238} \times (d-Z_2)^{-0.129} \times (Z_1-d)^{-0.152} \times d^{2.664} \times D^{0.955} \times \sigma_{0.2}^{0.058} \times E^{0.173}$	(2)
	K_p	*kN.m/rad*	$1.223 \times 10^{-5} \times t_p^{0.39} \times t_{fc}^{0.225} \times g^{-0.25} \times (d-Z_2)^{-0.1} \times (Z_1-d)^{-0.125} \times d^{2.852} \times D^{0.6432} \times \sigma_{0.2}^{0.0742} \times \sigma_u^{0.0208}$	(3)
	M_o	*kN.m*	$2.966 \times 10^{-4} \times t_p^{1.0238} \times g^{-0.11} \times (d-Z_2)^{-0.1274} \times (Z_1-d)^{-0.18} \times d^{1.04506} \times D^{1.171} \times \sigma_{0.2}^{0.42}$	(4)
	N	*dimensionless*	$2.6 \times 10^{-3} \times t_p^{0.904} \times t_{fc}^{0.377} \times g^{-0.214} \times (d-Z_2)^{-0.24} \times (Z_1-d)^{-0.209} \times d^{0.492} \times D^{-0.592} \times \sigma_{0.2}^{0.948}$	(5)

[Note]: Dimensions are expressed in mm, while material properties are measured in N/mm^2

Table 2: Evaluation of the analytical model in calculating K_i, K_p, M_o and N

	Statistical parameters	$\frac{K_{i,FE}}{K_{i,Analytical}}$	$\frac{K_{p,FE}}{K_{p,Analytical}}$	$\frac{M_{o,FE}}{M_{o,Analytical}}$	$\frac{N_{FE}}{N_{,Analytical}}$	No. of verifications
Unstiffened	Average	0.999	1.018	0.992	0.993	66
	COV (%)	9.8	9.9	7.5	6.1	

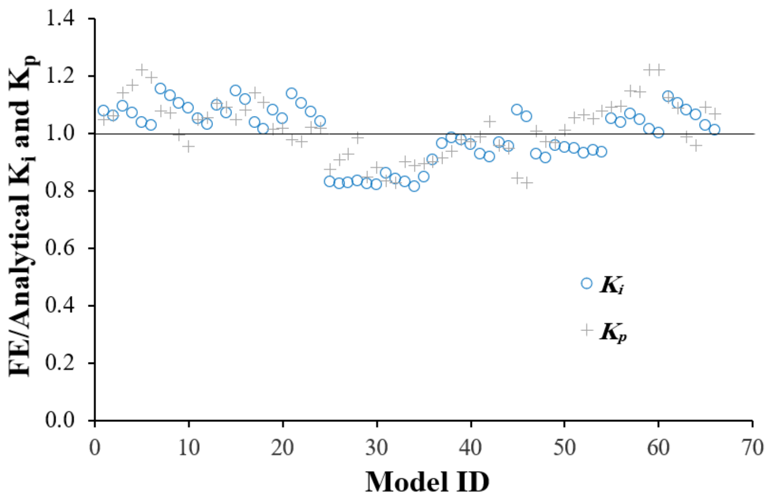

(a) K_i and K_p

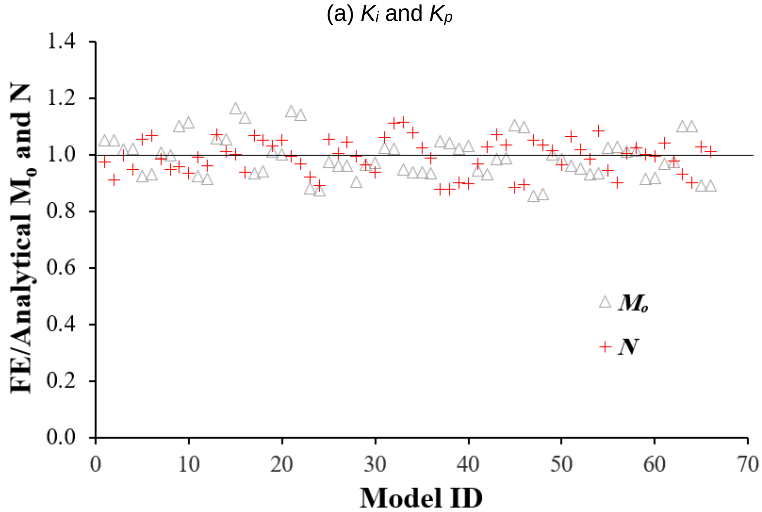

(b) M_o and N

Figure 2: Numerical and analytical four parameters for the 66 cases used to calibrate the model

3.3 Prediction of complete M-Φ curves

Based on Richard-Abbott formula (Equation 1) and on the four parameters analytically-determined (in the former subsection) for 66 stainless steel EEP joints, the complete analytical *M-Φ* responses for these connections were generated and then compared with their FE responses. Figure 3 and Table 3 illustrate comparisons of numerical and analytical outcomes for three different connections. It is noteworthy that, since there is no equation restricting the development of the analytical curves, they were projected until ultimate rotations estimated from numerical data, as shown in Figure 3. This limitation in the proposed analytical method will be discussed in detail in Section 3.4.

From the table and the figure, it is evident that there is an excellent correlation between the analytical and numerical moment-rotation curves. For all cases, there was no obvious discrepancy between the numerically- and analytically-generated results in the elastic portion of curves, whilst slight differences can be seen in a few cases at the plastic range of response.

3.4 Ultimate rotation function: development and verification

As shown in Section 3.3, the proposed analytical method (Equations 2 to 5) demonstrated great accuracy in predicting the *M-Φ* curves of connections, however, it had an obvious limitation; the analytical curves can progress interminably with no specific maximum moment/rotation. To address this limitation, a formula for the maximum moment or the rotation corresponding to it should be developed.

Utilizing nonlinear regression analysis of numerical data, a formula for the maximum rotation of stainless steel EEP connections was formulated in terms of the same geometrical and material properties previously used to develop the four parameters equations. The formulated maximum rotation function is shown in Table 4.

Based on the proposed equation, the ultimate rotation of the 66 stainless steel EEP connections were determined, and then verified using numerical results. Table 5 presents an assessment of the accuracy of the maximum rotation formula, showing a good agreement between the analytical and FE data, which indicates that the formulated maximum rotation function can address the above-mentioned limitation of Equations 2 to 5.

Table 3: Numerical and analytical results for three stainless steel EEP joints

Model ID	$\frac{K_{i,Analytical}}{K_{i,FE}}$	$\frac{K_{p,Analytical}}{K_{p,FE}}$	$\frac{M_{o,Analytical}}{M_{o,FE}}$	$\frac{N_{,Analytical}}{N_{,FE}}$
Model-08	0.88	0.93	1.00	1.06
Model-28	1.20	1.01	1.11	1.00
Model-59	0.99	0.82	1.10	1.00

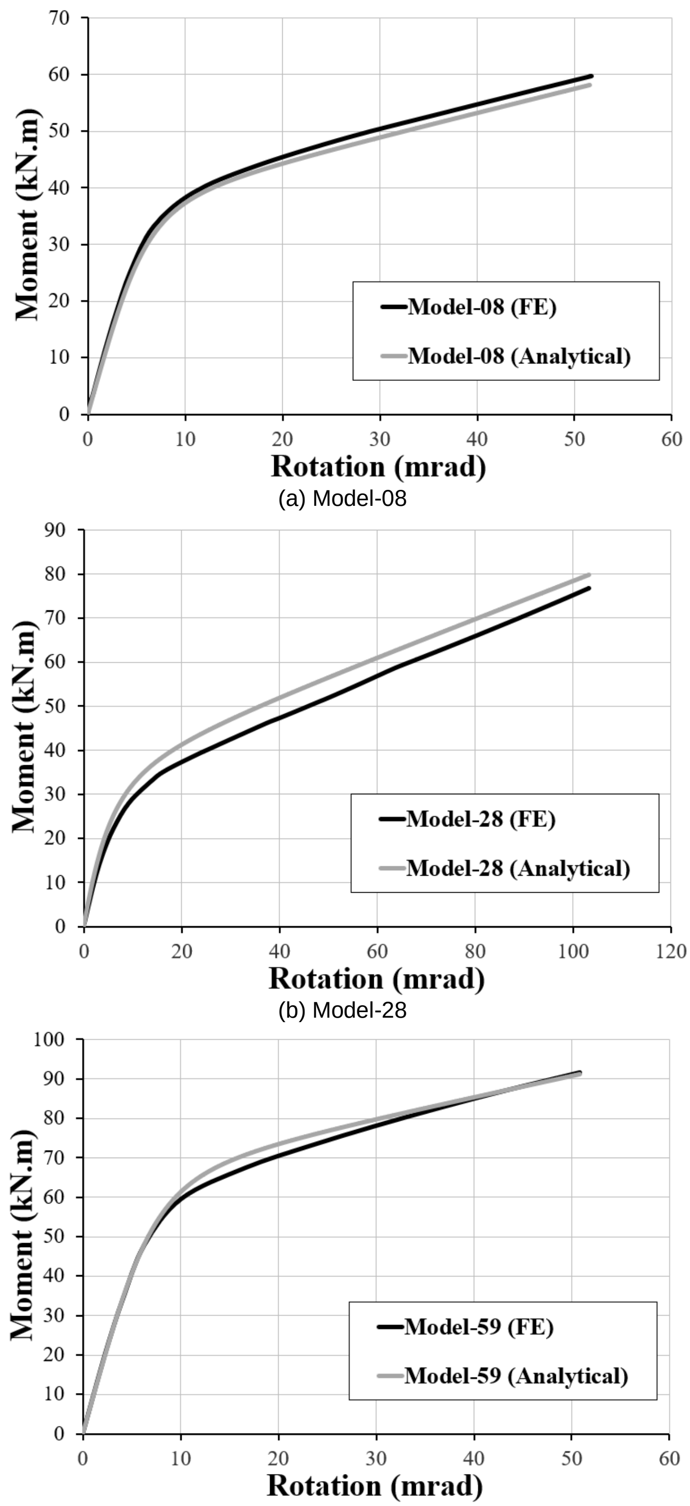

(a) Model-08

(b) Model-28

(c) Model-59

Figure 3: Comparison of finite element and analytical moment-rotation responses (projected until ultimate rotations estimated from finite element data)

Table 4: Maximum rotation formula suggested for unstiffened stainless steel EEP connections

	Parameter	Unit	Function	
Unstiffened	$\Phi_{j,u}$	*rad*	$0.60849 \times t_p^{-1.0049} \times t_{fc}^{-0.2978} \times g^{0.253} \times (d\text{-}Z_2)^{0.559} \times (Z_1\text{-}d)^{0.1255} \times d^{-1.033} \times D^{1.21} \times \sigma_{0.2}^{-0.0995}$	(6)

[Note]: Dimensions are expressed in mm, while material properties are measured in N/mm^2

Table 5: Assessment of the suggested equations in estimating maximum rotation ($\Phi_{j,u}$)

	Statistical parameters	$\frac{\Phi_{j,u,FE}}{\Phi_{j,u,Analytical}}$	No. of verifications
Unstiffened	Average	1.003	66
	COV (%)	9.1	

3.5 Prediction of maximum moment resistance

Using Richard-Abbott equation (Equation 1); the four parameters' expressions (Equations 2 to 5); and the formula proposed for the ultimate rotation (Equation 6), the maximum moment resistance for the 66 joints used in the development of the analytical model, was determined and validated against the corresponding FE data.

Figure 4 illustrates the FE and analytical maximum moments for the 66 cases. As shown in the figure, an excellent correlation can be seen between the FE and the analytical maximum moments ($M_{j,max}$). The average error (for all the analyzed joints) in calculating $M_{j,max}$ was about 4.6%, while the maximum error was under 10%. These minor differences show the apparent effectiveness of the suggested equations.

The complete analytical *M-Φ* curves for the connections were compared once again with numerical ones (they were compared earlier in Section 3.3). However, this time the analytical responses were plotted until analytically-estimated maximum rotations, as depicted in Figure 5. From the figure, it can be observed that a close correspondence was achieved between the analytical and numerical maximum resistance and moment-rotation responses.

3.6 Additional validation

In this subsection, the proposed analytical equations is further assessed by numerical data for joint configurations different from those used to calibrate the suggested model. A total of 12 cases, with geometric properties other than those explored in the former subsections, were considered, in order to examine the accuracy of the suggested model over a different range of parameters' values.

The columns and beams in all connections investigated in the additional validation had a depth, flange width, and web thickness of 300 mm, 200 mm; and 8 mm respectively, while the flange thickness was 12 mm in the case of beams and varied for the columns, as listed in Table 6 which displays the values of the parameters considered in this further verification.

Table 7 and Figure 6 compare the analytical and numerical key results (i.e. initial stiffness; maximum moment; rotation corresponding to maximum moment; and global *M-Φ* curves) for connections examined in the additional validation, while Figure 7 illustrates an assessment of the proposed model's capability to estimate the moment resistance for the additional joint configurations. From the table and the figures, the proposed simple method continued to yield accurate estimations for the moment-rotation behavior of unstiffened stainless steel EEP connections. The average error in calculating the ultimate moment for the 12 additional joints was approximately 7.5%, while the ultimate error did not overtake 10%. Considering the complex contact relationships and the nonlinear material behavior inherent in the investigated type of connection, it can be said that the accuracy of the suggested straightforward technique is acceptable for structural applications.

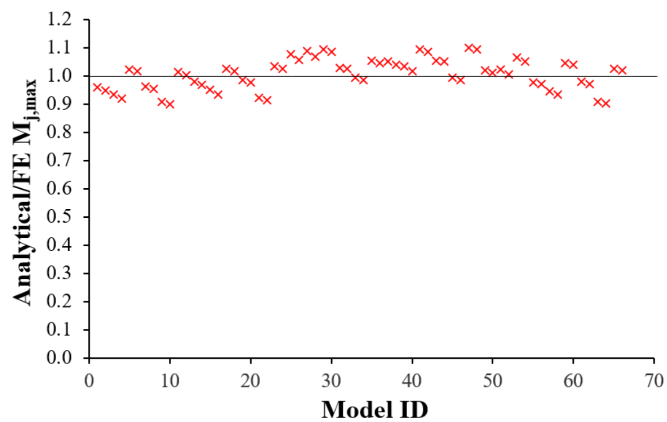

Figure 4: Comparison of numerical and analytical maximum moment resistance for the 66 connections considered in the current study

Table 6: Values of geometric and material properties investigated in the additional validation

t_p (mm)	t_{fc} (mm)	g (mm)	Z_1 (mm)	Z_2 (mm)	d (mm)	D (mm)	Stainless steel grade
12/14/16	12/16	108	344	232	300	16/20	EN 1.4301

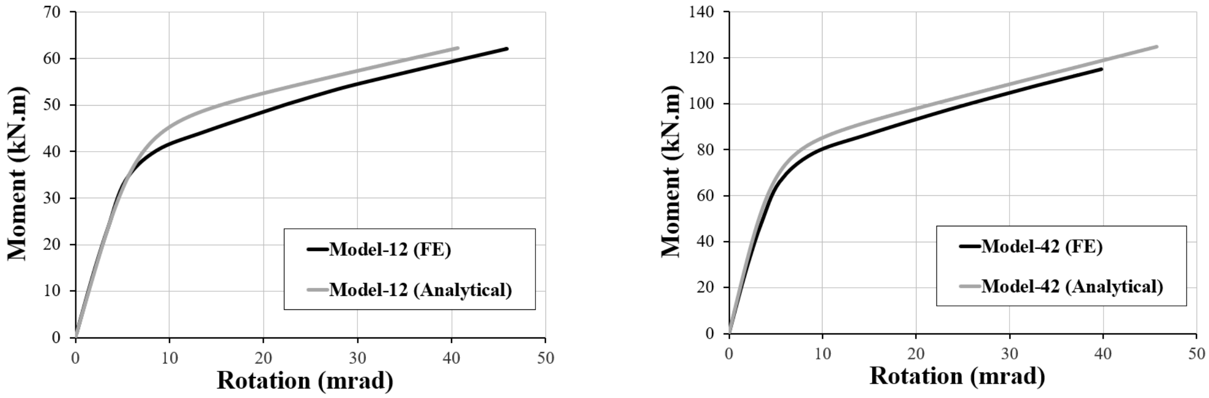

(a) Model-12 (b) Model-42

Figure 5: Numerical and analytical moment-rotation responses (the analytical curves are projected up to maximum rotations estimated analytically)

Table 7: Comparison of FE and analytical results for additional models investigated in the further verification

Model ID	$\frac{K_{i,Analytical}}{K_{i,FE}}$	$\frac{M_{j,max,Analytical}}{M_{j,max,FE}}$	$\frac{\Phi_{j,u,Analytical}}{\Phi_{j,u,FE}}$
Model-68	1.02	0.91	0.98
Model-77	0.99	0.96	1.07

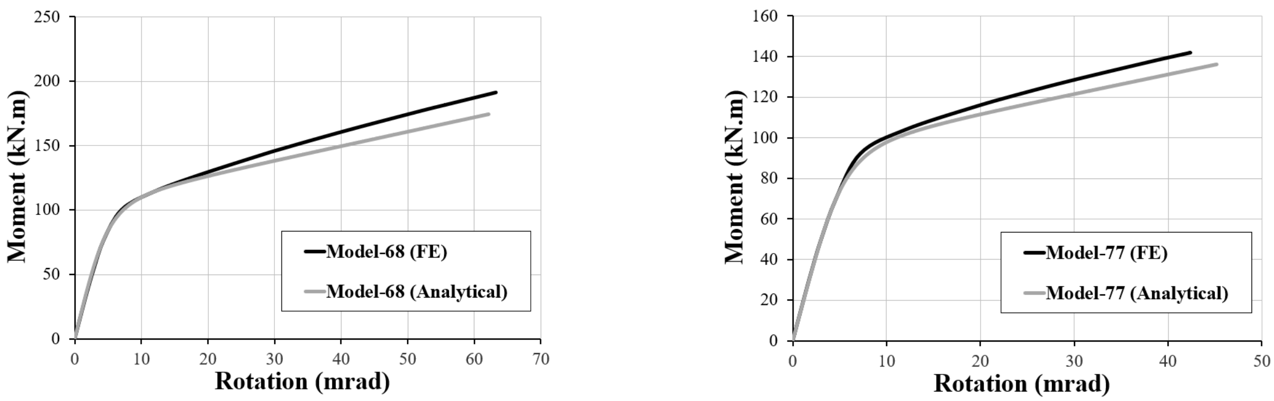

(a) Model-68 (b) Model-77

Figure 6: Comparison of FE and analytical moment-rotation curves for joints examined in the further verification

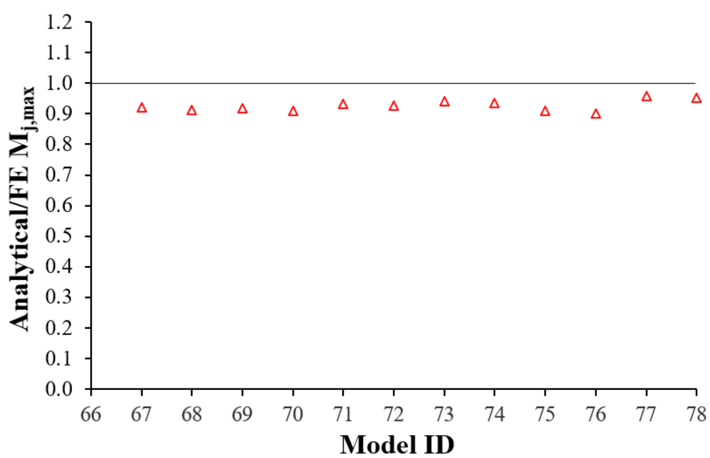

Figure 7: Evaluation of the analytical model in estimating the maximum moments of joints investigated in the additional validation (Models 67-78)

4. Conclusions

Using the FE data for 66 stainless steel unstiffened extended end-plate joints, a simple analytical model for predicting the moment-rotation behavior of such joints was suggested. A set of analytical formulas was developed, taking into consideration the considerable ductility of austenitic grades. By verifying the analytical data using numerical results, it was obvious that the suggested method is able to yield accurate predictions for the entire moment-rotation response. For the 66 cases, the average discrepancy between the FE and analytical maximum moment was about 4.6%. Moreover, further verification of the suggested equations was carried out depending on numerical results for joint configurations different from those employed to develop the analytical model. The additional validation demonstrated the high accuracy of the derived formulas in predicting the complete M-Φ curves of connections and in estimating their key parameters including initial stiffness and ultimate resistance. The maximum error in calculating the moment capacity for the 78 connections studied (including 66 joints used in the model's calibration in addition to 12 connections in the additional validation) was under 10%. This reasonable accuracy besides the straightforwardness of the proposed technique can greatly support its use in future academic and practical applications.

References

[1] Sakurai, S., Ellingwood, B. R. and Kushiyama, S. (2001) 'Probabilistic study of the behavior of steel frames with partially restrained connections', *Engineering Structures* 23 (11) 1410-1417. doi: 10.1016/S0141-0296(01)00052-9.

[2] Eladly, M. M. (2017) 'Numerical study on masonry-infilled steel frames under vertical and cyclic horizontal loads', *Journal of Constructional Steel Research* 138 308-323. doi: 10.1016/j.jcsr.2017.07.016.

[3] Sakr, M. A., Eladly, M. M., Khalifa, T. and El-Khoriby, S. (2019) 'Cyclic behaviour of infilled steel frames with different beam-to-column connection types', *Steel and Composite Structures* 30 (5) 443-456. doi: 10.12989/scs.2019.30.5.443.

[4] Errera, S.J. *et al.* (1974) 'Bolted and welded stainless steel connections', *Journal of Structural Engineering ASCE* 100 (6). 1279-1296.

[5] Soo Kim, T. and Kuwamura, H. (2007) 'Finite element modeling of bolted connections in thin-walled stainless steel plates under static shear', *Thin-Walled Structures* 45 (4) 407-421. doi: 10.1016/j.tws.2007.03.006.

[6] Salih, E. L., Gardner, L. and Nethercot, D. A. (2011) 'Bearing failure in stainless steel bolted connections', *Engineering Structures* 33 (2) 549-562.

[7] Feng, R. and Young, B. (2012) 'Design of cold-formed stainless steel tubular joints at elevated temperatures', *Engineering Structures* 35 188-202. doi: 10.1016/j.engstruct.2011.10.029.

[8] Feng, R. and Young, B. (2015) 'Theoretical analysis of cold-formed stainless steel tubular joints', *Engineering Structures* 83 99-115. doi: 10.1016/j.engstruct.2014.10.030.

[9] Feng, R., Lin, J. and Mou, X. (2019) 'Experiments on hybrid tubular K-joints with circular braces and square chord in stainless steel', *Engineering Structures* 190 52-65. doi: 10.1016/j.engstruct.2019.04.005.

[10] Hasan, M. J., Ashraf, M. and Uy, B. (2017) 'Moment-rotation behaviour of top-seat angle bolted connections produced from austenitic stainless steel', *Journal of Constructional Steel Research* 136 149-161. doi: 10.1016/j.jcsr.2017.05.014.

[11] Elflah, M. *et al.* (2019) 'Behaviour of stainless steel beam-to-column joints — Part 1: Experimental investigation', *Journal of Constructional Steel Research* 152 183-193. doi: 10.1016/j.jcsr.2018.02.040.

[12] Elflah, M., Theofanous, M. and Dirar, S. (2019) 'Behaviour of stainless steel beam-to-column joints-part 2: Numerical modelling and parametric study', *Journal of Constructional Steel Research* 152 194-212. doi: 10.1016/j.jcsr.2018.04.017.

[13] CEN (2006) 'BS EN 1993-1-4:2006 - Eurocode 3 - Design of steel structures - Part 1-4: General rules - Supplementary rules for stainless steels', *Eurocode 3*.

[14] EN 1993-1-8. (2005) 'Eurocode 3: Design of Steel Structures - Part 1.8: Design of Joints.', *CEN, Brussels*.

[15] Wang, M. *et al.* (2013) 'Numerical study on seismic behaviors of steel frame end-plate connections', *Journal of Constructional Steel Research* 90 140-152. doi: 10.1016/j.jcsr.2013.07.033.

[16] El-Khoriby, S., Sakr, M. A., Khalifa, T. and Eladly, M. M. (2017) 'Modelling and behaviour of beam-to-column connections under axial force and cyclic bending', *Journal of Constructional Steel Research* 129 171-184. doi: 10.1016/j.jcsr.2016.11.006.

[17] Eladly, M. M. (2020) 'Behaviour of stainless steel beam-to-column bolted connections–Part 1: Simplified FE model', *Journal of Constructional Steel Research*. 164 doi: 10.1016/j.jcsr.2019.105784.

[18] ABAQUS (2012) *User's Manual, Version 6.12*, *Simulia, Providence, RI*.

[19] Rasmussen, K. J. R. (2003) 'Full-range stress-strain curves for stainless steel alloys', *Journal of Constructional Steel Research* 59 (1) 47-61. doi: 10.1016/S0143-974X(02)00018-4.

[20] Richard, R. M. and Abbott, B. J. (1975) 'Versatile elastic-plastic stress-strain formula', *Journal* of the *Engineering* Mechanics *Division*. 101 (4) 511-515